Available online at www.sciencedirect.com
ScienceDirect
Atmospheric Environment 42 (2008) 970–979
ATMOSPHERIC ENVIRONMENT
www.elsevier.com/locate/atmosenv

Total gaseous mercury concentrations in ambient air in the eastern slope of Mt. Gongga, South-Eastern fringe of the Tibetan plateau, China

Xuewu Fu[a,b], Xinbin Feng[a,*], Wanze Zhu[c], Shaofeng Wang[a], Julia Lu[d]

[a]*State Key Laboratory of Environmental Geochemistry, Institute of Geochemistry, Chinese Academy of Sciences, Guiyang 550002, PR China*
[b]*Graduate University of the Chinese Academy Sciences, Beijing 100049, PR China*
[c]*Institute of Mountain Hazards and Environment, Chinese Academy of Sciences, Chengdu 610041, PR China*
[d]*Department of Chemistry and Biology, Ryerson University, Toronto, Ont., Canada M5B 2K3*

Received 13 February 2007; received in revised form 5 October 2007; accepted 8 October 2007

Abstract

During May 2005–June 2006, measurements of total gaseous mercury (TGM) concentrations were carried out by using a set of automatic atmospheric mercury vapor analyzer (Tekran 2537A) at Moxi base station (102°07′E, 29°40′N, 1640 m a.s.l.) of the Gongga alpine ecosystem observation and experiment station of Chinese academy of sciences (CAS) which belongs to the Chinese ecosystem research network (CERN). A seasonal distribution pattern of TGM in ambient air was observed on the descending order of winter, fall, spring, and summer. Geometric mean TGM concentration over the sampling periods was 3.98 ng m^{-3} with a range from 0.52 to 21.03 ng m^{-3}. The measurements showed a noticeable diurnal TGM distribution pattern with high concentration during daytime compared to nighttime; the maximum and the minimum concentration appeared near solar noon and immediately before sunrise, respectively. TGM concentrations were regulated by the wind directions, and wind from the southeastern direction carried more mercury than any other direction suggesting that anthropogenic sources, such as local zinc smelting activities and fuel combustion, played a predominant role in the elevation of TGM concentrations in this area.

Keywords: Total gaseous mercury (TGM); Atmosphere; Mt. Gongga; Southwest of China

1. Introduction

Total gaseous mercury (TGM) (mainly comprised of Hg^0) is the predominant form of atmospheric mercury (Slemr et al., 1985), which has long been depicted as a global pollutant because of its long residence time (0.5–2 yr) in the atmosphere (Schroeder and Munthe, 1998). Once being emitted from anthropogenic and natural sources, Hg^0 can be transported and deposited to remote places even 1000 km away from sources (Johansson et al., 2001). Mercury could undergo physical and chemical form transformation, and eventually be converted to methyl-mercury, a highly toxic mercury species that can pose seriously potential harm to human beings (Lindqvist, 1991). Anthropogenic sources which

*Corresponding author. Tel.: +86 851 5891356; fax: +86 851 5891609.
E-mail address: fengxinbin@vip.skleg.cn (X. Feng).

1352-2310/$ - see front matter © 2007 Elsevier Ltd. All rights reserved.
doi:10.1016/j.atmosenv.2007.10.018

include, coal combustion, waste incineration, metal smelting and production and cement production release large amounts of Hg^0 in addition to reactive gaseous mercury (RGM) and particulate mercury (PM) (Wilson et al., 2006); while natural sources, such as emissions from naturally mercury enriched soil, ocean surface, volcanoes and geothermal activities, predominantly emit Hg^0 (Moore and Carpi, 2005; Poissant et al., 1999; Gustin and Stamenkovic, 2005; Gustin, 2003).

Recent studies suggested that the mercury emission rates from anthropogenic activities seemed to decrease in Europe and North America via long term observations of atmospheric mercury concentrations during the last decade (Slemr and Scheel, 1998; Slemr et al., 1995, 2003; Iverfeldt et al., 1995). However, it is still difficult to predicate the worldwide trend of anthropogenic mercury emission rate because of the increased amount of coal combustion in developing countries (Jaffe et al., 2005; Pacyna et al., 2006), where the mercury emission inventories are poorly studied. Concentrations of TGM have been well documented at remote places in Europe and North American (Lindberg and Stratton, 1998; Poissant and Hoenninger, 2004; Poissant et al., 2005; Gabriel et al., 2005; Kellerhals et al., 2003; Wängberg et al., 2001), and background levels of TGM in North hemisphere are believed to be 1.5–2.0 ng m^{-3}. The profile of TGM concentrations, however, differs greatly among different continents due to combined effects of several factors such as diversity of source processes, fossil fuel use patterns and large-scale meteorological conditions (Pirrone et al., 1996). China is regarded as one of the largest anthropogenic mercury emission region in the world (Streets et al., 2005; Wu et al., 2006), but only a few measurements of TGM concentrations in ambient air of China to our best knowledge have been performed (Liu et al., 2002; Feng et al., 2003, 2004; Kuo et al., 2006). Most measurements were conducted only in urban areas and carried out for a relatively short period of time (Liu et al., 2002; Feng et al., 2003; Kuo et al., 2006). The current data on TGM concentrations in ambient air are not sufficient enough to elucidate the spatial and temporal distribution pattern of TGM in China. Moreover, there is no information about ambient TGM concentrations at relatively remote sites in China even though it has been reported that there are large differences in TGM concentrations between urban and remote areas. In this study, TGM concentrations in the ambient air were conducted at one site in the eastern slope of Mt. Gongga during the period from May 2005 to June 2006. The objectives of this study were to characterize the temporal distributions of the TGM concentrations in ambient air at a less human activities effected site in Southwestern China and to identify factors influencing the TGM distributions in this region.

2. Method

2.1. Monitoring site

Mt. Gongga (29°20′–30°20′ N, 101°30′–102°15′ E) is situated on the Quaternary sections of the eastern Qinghai-Tibet Plateau and its transit zone to the Sichuan province, and is the highest mountain in Sichuan province with the summit of 7556 m above sea level. The sampling site is located at the alpine ecosystem observation and experiment station (1640 m a.s.l.), which is also one of the background air pollutant monitoring stations operated by Chinese Academy of Sciences (CAS) (Fig. 1). The site is a flat alluvial plateau surrounded by alpine primary forest. The station is located in the northwest of Moxi town, and is equipped with standard meteorological instrumentations for temperature, relative humidity, wind direction, wind speed and solar radiation measurements. Meanwhile, airborne pollutants such as O_3, SO_2, NO_x are also monitored. The inlet of heated Teflon sampling tubing for TGM monitoring was mounted at 6 m above the ground.

Moxi town is located on about 200 km Southwestern of Chengdu and 42 km southern of Kangding city. Its population is about 7000, and annual coal consumption is about 900 tons. A village with population about 2000 is located 5 km northwest of the sampling site. There are no large-scale industrial activities in this area, while domestic coal and biofuel burning for cooking and house heating, gasoline consumption on motor vehicles are the main anthropogenic airborne mercury emission sources. Besides, it is worth noticing that two large counties are located on the southeastern of the sampling site. Shimian county situated 50 km southeast of sampling site with a population of 120,000, and Hanyuan county situated 60 km southeast of sampling site with a population of 340,000 are large zinc production areas and the annual Zn production of Shimian county reached about 100,000 tons. Zinc smelting could be an important atmospheric mercury emission source due to poor pollution control technologies applied (Feng et al., 2004; Streets et al., 2005).

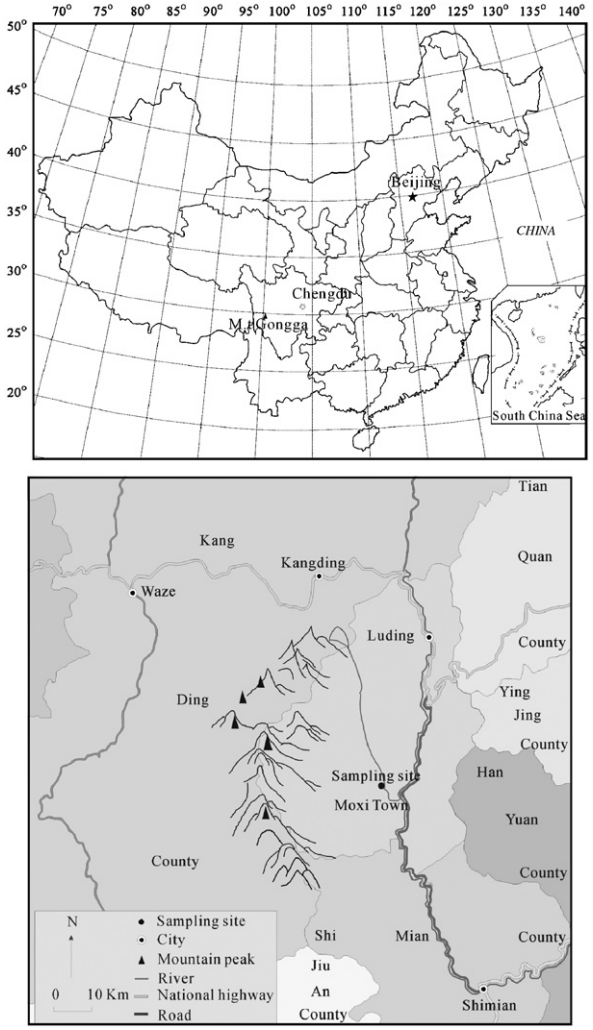

Fig. 1. Location of sampling site in the eastern slope of Mt. Gongga.

Because of the barrier effect of Mt. Gongga, no seasonal ground wind fields exist in the study area, and the wind system near the surface is mainly dominated by valley wind system regardless of seasons. In the daytime, air mass is mainly from southeastern direction and Hg polluted air in Shimian and Hanyuan counties may be transported to the sampling site; while during the nighttime, wind from the northwestern mountain side is dominant.

2.2. Automated TGM measurements

Measurements of the TGM concentrations in ambient air were performed with an automated mercury vapor analyzer Tekran Model 2537A (Schroeder et al., 1995). This analyzer is widely used all over the world and has demonstrated its accuracy, stability and reliability under most remote and rugged conditions imaginable (Tekran, 2002). Its technique is based on the collection of TGM on gold traps, followed by thermally desorption and finally detected as Hg^0 by cold vapor atomic fluorescence spectrometry ($\lambda = 253.7$ nm). A 45 mm diameter Teflon filter (pore size 0.2 μm) was used to protect the sampling cartridges against contamination of airborne particulate matters. The data quality of Tekran Model 2537A was guaranteed via periodical internal recalibration with a 25 h interval and the internal permeation source was calibrated every 2 months. The precision of Tekran Model 2537A is less than 2% and the detection limit is less than 0.1 ng m^{-3}, and this provided analysis of TGM in the air at sub-ng m^{-3} levels (Tekran, 2002). The sampling flow rate was set at 1.5 L min^{-1} and the sampling time was 5 min except during the sampling period from 4 January to 7 April 2006 in which a sampling time of 15 min was applied.

In this study, we intended to measure TGM concentrations on routine basis; however, there were still some interruptions caused by the instrument maintenance and the employment of the analytical system on other study purposes. The longest periods which we were unable to retrieve data included the following 6 terms: (1) 11–17 June 2005; (2) 6–13 September 2005; (3) 30 September to 11 October 2005; (4) 29 November to 6 December 2005; (5) 4 March to 7 April 2006; and (6) 12–16 April 2006. Except for these breaking periods, we collected a total of 53532 individual data points from our TGM measurements.

3. Results and discussion

3.1. Overall TGM distribution characteristics in the study site

Fig. 2 represents the highly-time resolved long-term data set of TGM concentrations in ambient air at Moxi sampling site, and the geometric mean TGM concentration (because TGM data followed a log normal distribution pattern as discussed later in this section, the geometric mean will best present the average concentration) over the sampling period was 3.98 ng m^{-3} with the range across two orders of magnitude from 0.52 to 21.03 ng m^{-3} (Table 1). TGM concentrations in ambient air in our study area were much lower than those observed in some

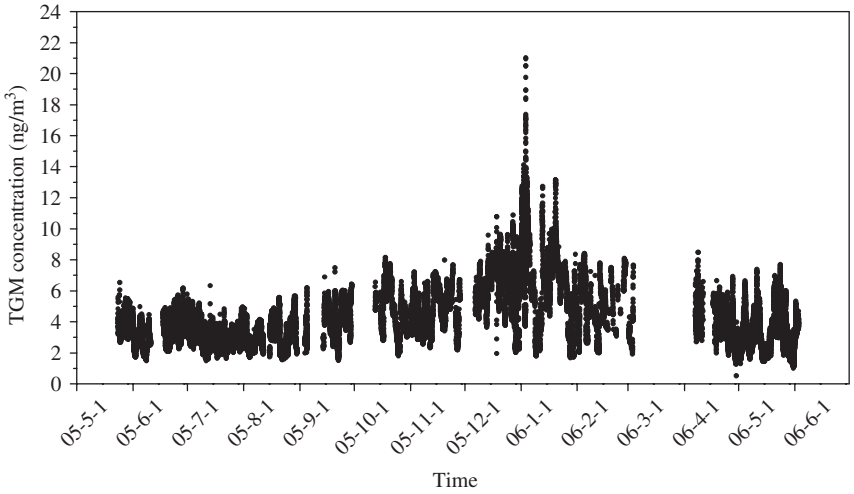

Fig. 2. Total gaseous mercury (TGM) concentration in the ambient air at Moxi sampling site.

Table 1
Statistic summary of TGM concentrations ($ng\,m^{-3}$) at Moxi sampling site

	Maximum	Minimum	Geomean	SD	Median	*n*
Spring (March–May)	8.49	0.52	3.37	1.20	3.55	14 361
Summer (June–August)	6.33	1.49	3.02	0.63	3.12	22 096
Autumn (September–November)	8.14	1.52	4.35	1.40	4.56	7733
Winter (December–February)	21.03	1.69	5.65	2.03	6.39	9342
All data	21.03	0.52	3.98	1.62	3.89	53 532

urban areas in China. Mean TGM concentration in ambient air at a residential area in Guiyang, Southwestern China was 8.40 $ng\,m^{-3}$ during the 1 year measurement campaign from November 2000 to November 2001 (Feng et al., 2004). Kuo et al. (2006) measured TGM concentrations at Chupei city, northwest of Taiwan, China and found that the mean TGM concentration was 8.40 $ng\,m^{-3}$. The mean TGM concentration measured at a residential area in Beijing reached up to 16.67 $ng\,m^{-3}$ and was about four times higher compared to our result. It is clear that the mean TGM concentration at Moxi sampling site is much higher than those observed in some remote areas in northern America and Europe. Burke et al. (1995) measured TGM concentrations at a number of remote areas in the Great Lakes region of North America and found the mean TGM concentrations were between 1.59 and 1.93 $ng\,m^{-3}$. Kim et al. (2005) analyzed both spatial and temporal distribution characteristics of atmospheric mercury using data collected from a period of 4–6 years at six sites in America, Asia, Arctic and Europe, and concluded that the annual mean TGM concentrations at all stations except for Seoul were between 1.58 and 1.93 $ng\,m^{-3}$, which clearly reflected the TGM concentrations in background areas in Northern hemisphere. The elevated TGM concentrations in Moxi sampling site reflected that the regional background level of TGM in southwestern china was elevated. Southwestern China is one of the largest mercury emission areas in China, and coal combustion related to industrial and domestic purposes together with non-ferrous metal (especially zinc) smelting activities are the two main mercury sources. It was reported that total mercury emission from Guizhou, Sichuan and Yunan provinces reached about 128 tons in 2003 (Wu et al., 2006), and the huge amount of mercury emissions definitely contributed to the elevation of TGM concentrations in this region. Meanwhile, local Hg emissions from large quantities fuel consumption and zinc smelting activities are also notable. The sampling site is located adjacently to Moxi town, and mercury emissions from local

human activities would inevitably contribute to the elevated TGM concentrations at the sampling site. Besides, mercury emissions from zinc smelting industries in Shimian and Hanyuan counties could also contribute to the elevated TGM concentrations at Moxi site. No data from the open literature was available on mercury emission from zinc smelting activities in Shimian and Hanyuan counties. If the average mercury emission factors for zinc smelting of 86.6 g t^{-1} was used to estimate mercury emission from zinc smelting in China (Streets et al., 2005), annual mercury emission from zinc smelting in Shimian county will reach 8.7 tons since the annual zinc production is about 100,000 tons. Moreover, these two counties are densely populated and mercury emissions from fuel consumption would also be considerable as well. Since Shimian and Hanyuan counties are located in the upper wind direction of the sampling site, mercury emission from these counties may probably be transported to Moxi sampling site and result in the elevation of TGM concentrations.

Frequency distributions of the high time resolved TGM data from the whole measurement campaign is shown in Fig. 3. TGM concentrations followed a typical log normal distribution pattern, and TGM concentrations dominantly fell in the range of 2–6 ng m^{-3}, which accounted for 76.02% of the total frequency. However, a large variability of the TGM concentrations was observed. Unusual high concentration data were abundant with 1.55% of the TGM data sets exceeding 10 ng m^{-3}, and most of which were seen dominantly during the winter months (December and January).

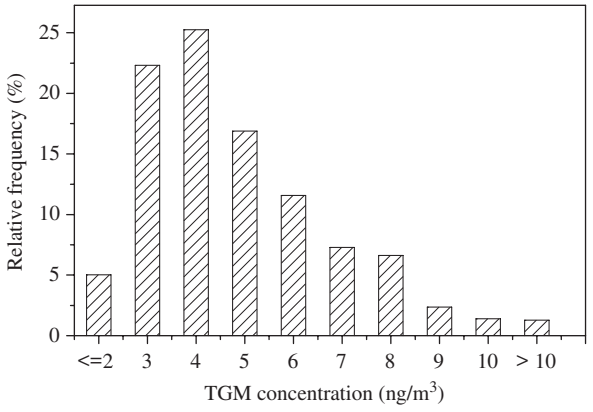

Fig. 3. Frequency distribution of TGM covered the whole sampling period at Moxi sampling site. The calculation is based on the hourly averaged TGM concentrations.

Southeastern and northwestern winds were the dominant winds during the whole sampling period (Fig. 4A), which accounted for 84.2% of the total frequency. The valley in which the sampling site is situated stretches along the southeastern and northwestern direction. The mean TGM concentrations in ambient air from any wind directions throughout the study period were obviously higher than the values observed in the background areas in Europe and North America (Fig. 4B), implying that the regional background TGM concentrations in the atmosphere were elevated. Wind from northwest direction traveling over the mountains before reaching the sampling site showed the lowest average TGM concentration of 3.52 ng m^{-3}; while southeast wind showed the highest average TGM concentration of 5.17 ng m^{-3}, suggesting that mercury emission from zinc smelting activities in Shimian and Hanyuan counties did have a strong impact on TGM distribution at the sampling site. Mean TGM concentration was 4.27 ng m^{-3} during these periods when no wind was detected. This value is some what higher than the average TGM concentrations observed from wind from the northwest direction,

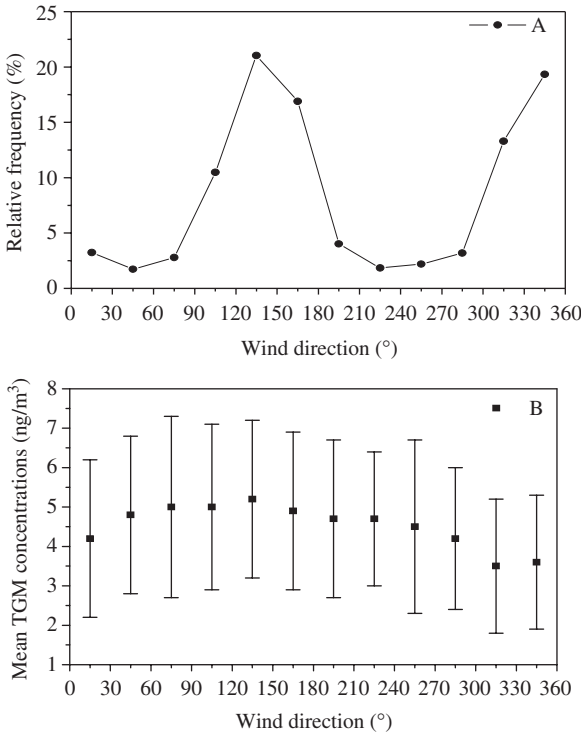

Fig. 4. Wind directional dependence of mean TGM concentrations and wind frequency distribution for the whole sampling period at Moxi sampling site.

suggesting that anthropogenic activities in Moxi town could contribute to the elevation of TGM concentrations observed in the sampling site to some degree.

3.2. Seasonal distribution patterns of TGM

To assess the seasonal variation of TGM concentrations, distribution of monthly geometric mean TGM concentrations at Moxi sampling site is shown in Fig. 5, and a remarkable seasonal distribution pattern was observed. The seasonal geometric mean TGM values decreased on the descending order: winter ($5.65\,ng\,m^{-3}$), autumn ($4.35\,ng\,m^{-3}$), spring ($3.37\,ng\,m^{-3}$), and summer ($3.02\,ng\,m^{-3}$). The highest monthly concentrations were observed in December 2005 with a geometric mean of $6.47\,ng\,m^{-3}$, which was more than two times higher than the lowest monthly geometric mean concentration of $2.92\,ng\,m^{-3}$ observed in June 2005. This seasonal pattern in fact can be regarded as the most common one in the northern hemispheric (Kim et al., 2005; Dastoor and Larocuue, 2004), and the summer minimum and winter maximum TGM concentrations were also observed in many previous studies (Ebinghaus et al., 2002; Kellerhals et al., 2003; Kock et al., 2005; Poissant et al., 2005). There were several possible reasons for this remarkable seasonal distribution pattern of TGM concentrations.

First of all, increase of TGM concentrations in wintertime was reasonable due to the enhancement of anthropogenic mercury emissions (Feng et al., 2004; Kim and Kim, 2000; Kellerhals et al., 2003). Feng et al. (2004) discussed the seasonal change of TGM in Guiyang city, southwestern China, and found that the increased domestic coal consumption for household heating was the main cause of elevated TGM concentrations observed in winter. Due to the maintenance of the instruments, we only have measurement data of SO_2 and NO_x for the period from 1 July to 12 November 2005 during our sampling campaign. The mean SO_2 and NO_x concentrations for this period were 2.43 and 1.95 ppb, respectively, which were elevated compared to those observed in remote areas in Europe (i.e. Reatad et al., 1998), indicating the existence of local coal combustion sources. Generally, coal combustion emission is one of the most important sources of atmospheric SO_2 and NO_x, and we did correlation analysis between TGM and these two airborne contaminants as shown in Fig. 6. No significantly positive correlations between TGM and both SO_2 and NO_x were observed during the period from 1 July to 12 November 2005 (Fig. 6a and c). This implies that the regional coal combustion sources contributed more to the elevation of these contaminants at the sampling site for the period from 1 July to 12 November 2005 compared to the local combustion sources from Moxi town because SO_2 and NO_x have much shorter lifetime in the atmosphere compared to TGM. However, significant correlations between TGM and both

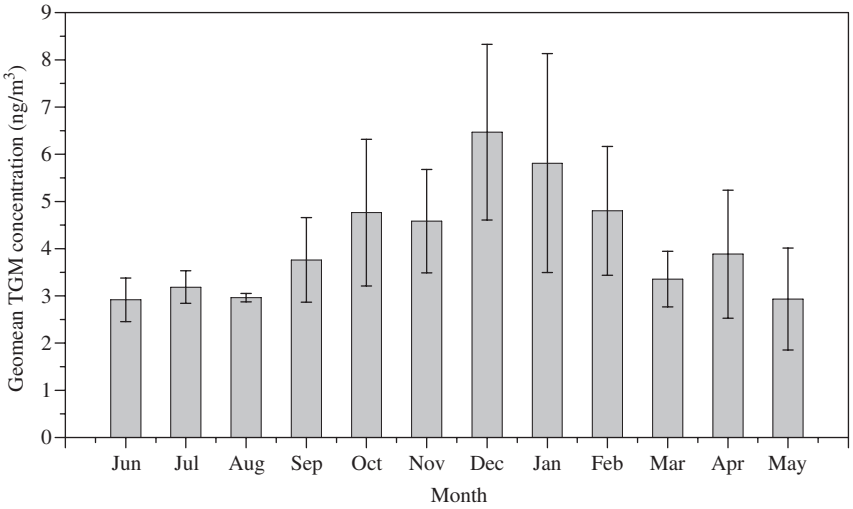

Fig. 5. Monthly geomean concentrations of TGM at Moxi sampling site based on hourly mean concentrations. Whiskers above and within the box indicate the standard deviations.

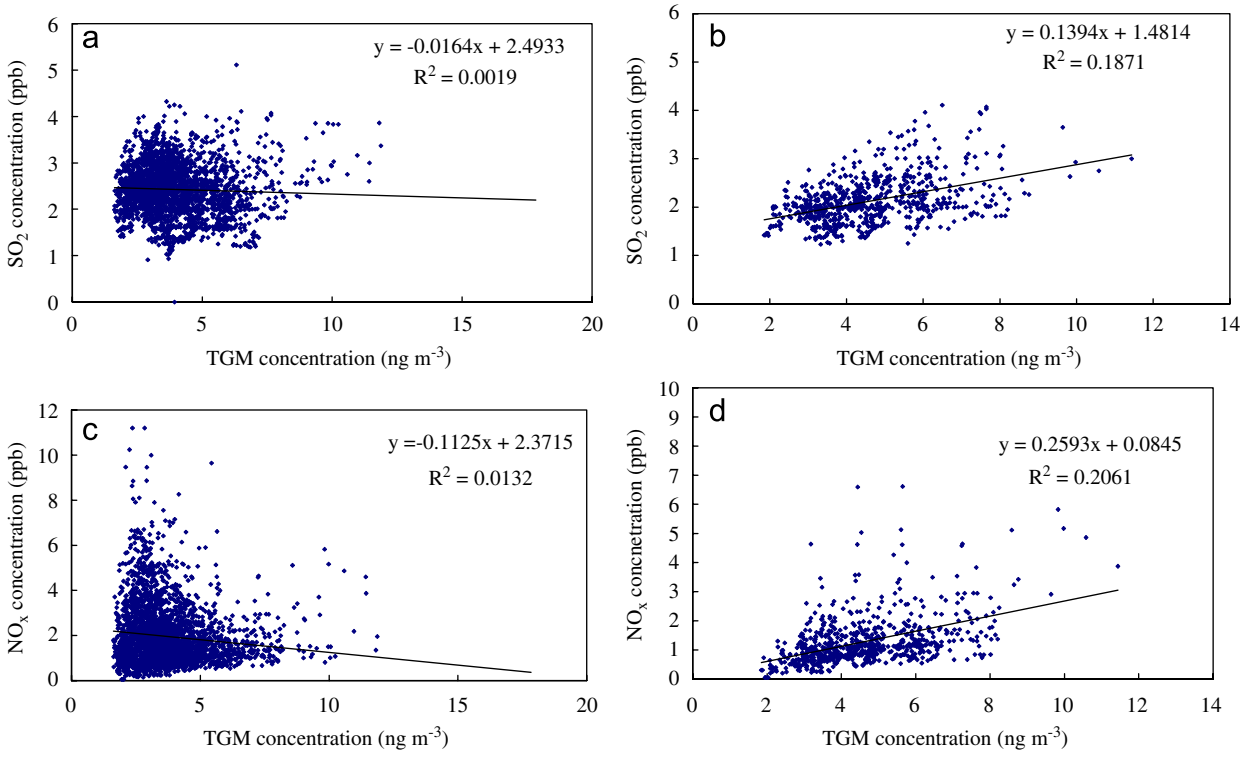

Fig. 6. The correlations between TGM and SO_2 and NO_x. (a) The correlation between TGM and SO_2 during the period from 1 July to 12 November 2005; (b) the correlation between TGM and SO_2 during the period from 12 October to 12 November 2005; (c) the correlation between TGM and NO_x during the period from 1 July to 12 November 2005; (d) the correlation between TGM and NO_x during the period from 12 October to 12 November 2005.

SO_2 and NO_x concentrations in ambient air were observed during the cold period from 12 October to 12 November 2005 as shown in Fig. 6b and d. The correlation coefficient between TGM and SO_2 was 0.43 ($P<0.001$) and that between TGM and NO_x was 0.45 ($p<0.001$). Since domestic coal burning for house heating activities initiated in that period of time, local coal burning activities significantly contributed to the elevation of TGM, SO_2 and NO_x at the sampling site. This line of evidence reinforced the argument that the local domestic coal burning for house heating was responsible for the elevated TGM concentrations in cold months.

On the other hand, seasonal variation of the reactions between atmospheric oxidants and Hg^0 might also play an important role in the seasonal distribution pattern of TGM. The major oxidation species in the troposphere is the OH radical, of which the concentrations varied seasonally, with summer and spring concentrations higher than autumn and winter values (Bahm and Khalil, 2004), and accelerated oxidation rate of Hg^0 by OH radical in summer and followed by dry deposition and wet scavenging process was an important reason attributed to the summer minimum TGM concentrations in the atmosphere (Bergan and Rodhe, 2001). Moreover, it is also well documented that the substantial dry deposition of TGM to forest leaves occurred in growing seasons (Rea et al., 2001) because it is clear that a major portion of the mercury in foliage originates from the atmosphere (Fleck and Grigal, 1998). As PM are likely to be washed-off from the foliar surface via throughfall, the majority of dry deposition to foliage is gaseous form which account for a large fraction of total mercury deposition (Rea et al., 2001). The foliar uptake of TGM during growing seasons (April–October) might result in more dry deposition of TGM during summer than the other seasons.

3.3. Diurnal variation of TGM concentrations

Annual hourly mean TGM concentrations at Moxi sampling site are shown in Fig. 7, and diurnal distribution pattern of TGM concentrations was obvious from this analysis. TGM concentrations

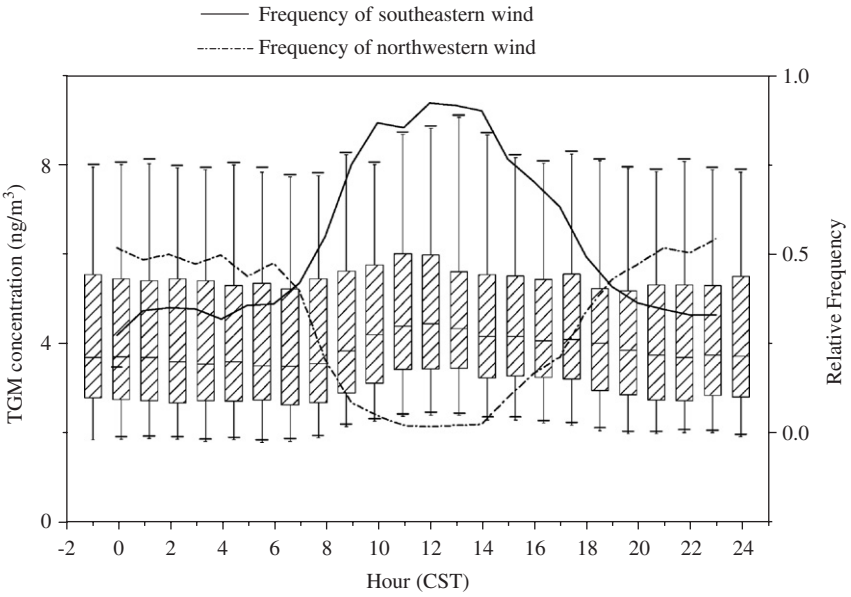

Fig. 7. Hourly median concentrations of TGM and the frequency of southeast and northwest wind at Moxi sampling site.

peaked at noon, and then decreased and the lowest concentration was observed in the early morning. The diurnal distribution pattern is quite similar to those observed at a suburban site in northeast Taiwan, China (Kuo et al., 2006). Kellerhals et al. (2003) also reported that seven of the 10 measurement sites in the Canadian atmospheric mercury measurement network (CAMNet) experienced a similar cycle of maximum concentrations near solar noon (10:00–14:00 local standard time) and minimum concentrations in early morning (03:00–07:00). A different diurnal TGM distribution pattern was observed at several European sites (Lee et al., 1998; Schmolke et al., 1999). In these sites, maximum TGM concentrations occurred in the night or early morning. These nighttime peaks of TGM concentrations were attributed to the fact that Hg^0 emitted from surface accumulated in the nocturnal inversion layer (Schmolke et al., 1999). In contrast, one of the most important reasons regulated the diurnal distribution pattern of TGM at Moxi sampling site was the transport process of TGM. As discussed above, the wind from southeast carried air mass with higher mercury concentrations than those from other directions. It is shown from Fig. 7 that TGM concentrations correlated significantly with the hourly relative frequencies of the southeastern wind occurrence ($r = 0.88$, $p < 0.001$). As stated previously, the dominant wind direction at the study site was mainly from the southeast and northwest (Fig. 7). The diurnal cycle of wind directions at the sampling site demonstrated a distinct characteristic of valley wind system, and the predominant wind in the daytime was from southeast, which contained elevated TGM concentrations. During the nighttime, wind from northwest direction was dominant, which brings clear air to the sampling site.

4. Conclusion

Geometric mean TGM concentration in ambient air at the study site was 3.98 ng m^{-3} with a range from 0.52 to 21.03 ng m^{-3}, which is significantly elevated compared to the values observed at global background sites in Europe and North America, which varied from 1.5 to 2.0 ng m^{-3}. A distinctly seasonal distribution pattern of TGM was observed during the measurement period. TGM concentrations were the highest in winter and the lowest during summer. The geometric mean TGM concentration in summer was 0.96 ng m^{-3} lower than the annual geometric mean value, while the mean value in winter was 1.67 ng m^{-3} higher than the annual mean. The diurnal distribution pattern was generally characterized by the elevated concentrations during daytime compared to nighttime and the maximum concentration occurred near the solar noon and the minimum concentration appeared immediately before sunrise. The wind directions

regulated TGM concentrations, and southeastern wind carried more mercury than any other directions. Obviously, the regional and local anthropogenic sources such as smelting activities and fuel combustion play a predominant role in the elevation of TGM concentrations in the air at the sampling site.

Acknowledgments

The study is financially supported by CAS through an innovation project (KZCX3SW-443), the Field Station Foundation, the International Partnership Project, and Natural Science Foundation of China (405320514).

References

Bahm, K., Khalil, M.A.K., 2004. A new model of tropospheric hydroxyl radical concentrations. Chemosphere 54, 143–166.

Bergan, T., Rodhe, H., 2001. Oxidation of elemental mercury in the atmosphere; constraints imposed by global scale modeling. Journal of Atmospheric Chemistry 40, 191–212.

Burke, J., Hoyer, M., Keeler, G., Scherbatskoy, T., 1995. Wet deposition of mercury and ambient mercury concentration at a site in the lake champlain basin. Water, Air and Soil Pollution 80, 353–362.

Dastoor, A.P., larocuue, Y., 2004. Global circulation of atmospheric mercury: a modelling study. Atmospheric Environment 38, 147–161.

Ebinghaus, R., Kock, H.H., Coggins, A.M., Spain, T.G., Jennings, S.G., Temme, C., 2002. Long-term measurements of atmospheric mercury at mace head, Irish west coast, between 1995 and 2001. Atmospheric Environment 36, 5267–5276.

Feng, X.B., Tang, S.L., Shang, L.H., Yan, H.Y., Sommar, J., Lindqvist, O., 2003. Total gaseous mercury in the atmosphere of guiyang, PR China. The Science of the Total Environment 304, 61–72.

Feng, X.B., Tang, S.L., Shang, L.H., Yan, H.Y., Zheng, W., 2004. Temporal variation of total gaseous mercury in the air of Guiyang, China. Journal of geophysical research 109, D03303.

Fleck, J.A., Grigal, D.F., 1998. Mercury uptake by trees: an observational experiment. Water, Soil and Air pollution 115, 513–523.

Gabriel, M.C., Williamson, D.G., Brooks, S., Lindberg, S.E., 2005. Atmospheric speciation of mercury in two contrasting Southeastern US airsheds. Atmospheric Environment 39, 4947–4958.

Gustin, M.S., 2003. Are mercury emissions from geologic sources significant? A status report. The Science of Total Environment 34, 153–167.

Gustin, M., Stamenkovic, J., 2005. Effect of watering and soil moisture on mercury emissions from soils. Biogeochemistry 76, 215–232.

Iverfeldt, Å., Munthe, J., Pacyna, J., Brosset, C., 1995. Long-term changes in concentrations and deposition of atmospheric mercury over Scandinavia. Water, Air and Soil Pollution 80, 227–233.

Jaffe, D., Prestbo, E., Swartzendruber, P., Penziasa, P.W., Kato, S., Takamid, A., Hatakeyamad, S., Kajii, Y., 2005. Export of atmospheric mercury from Asia. Atmospheric Environment 39, 3029–3038.

Johansson, K., Bergback, B., Tyler, G., 2001. Impact of atmospheric long range transport of lead, mercury and cadmium on the Swedish forest environment. Water, Air, and Soil Pollut. Focus 1, 279–297.

Kellerhals, M., Beauchamp, S., Belzer, W., Blanchard, P., Froude, F., Harvey, B., McDonald, K., Pilote, M., Poissant, L., Puckett, K., Schroeder, B., Steffen, A., Tordon, R., 2003. Temporal and spatial variability of total gaseous mercury in Canada: results from the Canadian atmospheric mercury measurement network (CAMNet). Atmospheric Environment 37, 1003–1011.

Kim, K.H., Kim, M.Y., 2000. The effects of anthropogenic sources on temporal distribution characteristics of total gaseous mercury in Korea. Atmospheric Environment 34, 3337–3347.

Kim, K.H., Ebinghaus, R., Schroeder, W.H., Blanchard, P., Kock, H.H., Steffen, A., Froude, F.A., Kim, M.Y., Sungmin, H., Kim, J.H., 2005. Atmospheric mercury concentrations from several observatory sites in the northern hemisphere. Journal of Atmospheric Chemistry 50, 1–24.

Kock, H.H., Bieber, E., Ebinghaus, R., Spain, T.G., Thees, B., 2005. Comparison of long-term trends and seasonal variations of atmospheric mercury concentrations at the two European coastal monitoring stations Mace Head, Ireland, and Zingst, Germany. Atmospheric Environment 39, 7549–7556.

Kuo, T.H., Chang, C.F., Urba, A., Kvietkus, K., 2006. Atmospheric gaseous mercury in Northern Taiwan. Science of Total Enviroment 368, 10–18.

Lee, D.S., Dollard, G.J., Pepler, S., 1998. Gas-phase mercury in the atmosphere of the United Kingdom. Atmospheric Environment 32, 855–864.

Lindberg, S.E., Stratton, W.J., 1998. Atmospheric speciation concentrations and behavior of reactive gaseous mercury in ambient air. Environmental Science and Technology 32, 49–57.

Lindqvist, O., 1991. Mercury in the Swedish environment: recent research on causes, consequences and corrective methods. Water Air and Soil Pollution 55, 1–261.

Liu, S.L., Nadim, F., Perkins, C., Carley, R.J., Hoag, G.E., Lin, Y., 2002. Atmospheric mercury monitoring survey in Beijing, China. Chemosphere 48, 97–107.

Moore, C., Carpi, A., 2005. Mechanisms of the emission of mercury from soil: role of UV radiation. Journal of geophysical research 110 (D24302), 1–9.

Pacyna, E.G., Pacyna, J.M., Steenhuisenc, F., Wilson, S., 2006. Global anthropogenic mercury emission inventory for 2000. Atmospheric Environment 40, 4048–4063.

Pirrone, N., Keeler, G.J., Nriagu, J.O., 1996. Regional differences in worldwide emissions of mercury to the atmosphere. Atmospheric Environment 30, 2981–2987.

Poissant, L., Hoenninger, G., 2004. Atmospheric mercury & ozone depletion events observed at the Hudson Bay in Northern Quebec along to BrO (DOAS) measurements. RMZ–Materials and Geoenvironment 51 (1), 1722–1725.

Poissant, L., Pilote, M., Casimir, A., 1999. Mercury flux measurements in a naturally enriched area: correlation with

environmental conditions during the nevada study and tests of the release of mercury from soils (STORMS). Journal of Geophysical Research Atmosphere 104, 21,845–21,858.

Poissant, L., Pilote, M., Beauvais, C., Constant, P., Zhang, H., 2005. A year of continuous measurements of three atmospheric mercury species (GEM,RGM and Hgp) in southern Qué bec,Canada. Atmospheric Environment 39, 1275–1287.

Rea, A.W., Lindberg, S.E., Keeler, G.J., 2001. Dry deposition and foliar leaching of mercury and selected trace elements in deciduous forest throughfall. Atmospheric Environment 35, 3453–3462.

Reatad, K., Isaksen, I.S.A., Berntsen, T.K., 1998. Global distribution of sulphate in the troposphere, a three-demensional model study. Atmospheric Environment 32 (20), 3593–3609.

Schroeder, W.H., Munthe, J., 1998. Atmospheric mercury: An overview. Atmospheric Environment 32, 809–822.

Schmolke, S.R., Schroeder, W.H., Kock, H.H., Schneeberger, D., Munthe, J., Ebinghaus, R., 1999. Simultaneous measurements of total gaseous mercury at four sites on a 800 km transect: spatial distribution and short-time variability of total gaseous mercury over central Europe. Atmospheric Environment 33, 1725–1733.

Schroeder, W.H., Lamborg, C., Schneeberger, D., Fitzgerald, W.F., Srivastava, B., 1995. Comparison of a manual method and an automated analyzer for determining total gaseous mercury in ambient air. In: Wilken, R. D., Förster, A., and Knöchel, U. (Eds.), Proceedings of the 10th International Conference on Heavy Metals in the Environment, vol. 2, CEP Consult. Ltd., Edinburgh, UK, pp. 57–60.

Slemr, F., Scheel, H.E., 1998. Trends in atmospheric mercury concentrations at the summit of the wank mountain,southern Germany. Atmospheric Environment 32, 845–853.

Slemr, F., Schuster, G., Seiler, W., 1985. Distribution, speciation, and budget of atmospheric mercury. Journal of Atmospheric Chemistry 3, 407–434.

Slemr, F., Junkermann, W., Schmidt, R.W., Sladkovic, R., 1995. Indication of change in global and regional trends of atmospheric mercury concentrations. Geophysical. Research. Letters 22, 2143–2146.

Slemr, F., Brunke, E.G., Ebinghaus, R., Temme, C., Munthe, J., Wängberg, I., Schoreder, W., Steeffen, A., 2003. Worldwide trend of atmospheric mercury since 1977. Geophysical Research Letters 30 NO10 (23), 1–4.

Street, D.G., Hao, J.M., Wu, Y., Jiang, J.K., et al., 2005. Anthropogenic mercury emission in China. Atmospheric Environment 39, 7789–7806.

Tekran, 2002. Model 2537A Mercury Vapour Analyzer User Manual, Toronto, Canada.

Wängberg, I., Munthe, J., Pirrone, N., Iverfeldt, Å., Bahlman, E., Costa, P., Ebinghaus, R., Feng, X., Ferrara, R., Gårdfeldt, K., Kock, H., Lanzillotta, E., Mamane, Y., Mas, F., Melamed, E., Osnat, Y., Prestbo, E., Sommar, J., Schmolke, S., Spain, G., Sprovieri, F., Tuncel, G., 2001. Atmospheric mercury distribution in Northern Europe and in the Mediterranean region. Atmospheric Environment 35, 3015.

Wilson, S.J., Steenhuisen, F., Pacyna, J.M., Pacyna, E.G., 2006. Mapping the spatial distribution of global anthropogenic mercury atmospheric emission inventories. Atmospheric Environment 40, 4621–4632.

Wu, Y., Wang, S.X., Streets, D.G., Hao, J.M., Chan, M., Jiang, J.K., 2006. Trends in anthropogenic mercury emissions in China from 1995 to 2003. Environmental Science and technology 40, 5312–5318.